Proc. Natl. Acad. Sci. USA
Vol. 79, pp. 6137–6141, October 1982
Biochemistry

Conformational flexibility in the active sites of aspartyl proteinases revealed by a pepstatin fragment binding to penicillopepsin

(enzyme structure/transition-state analogue/x-ray crystal structure)

MICHAEL N. G. JAMES*, ANITA SIELECKI*, FRANK SALITURO†, DANIEL H. RICH†, AND THEO HOFMANN‡

*Medical Research Council of Canada, Group in Protein Structure and Function, Department of Biochemistry, University of Alberta, Edmonton, Alberta, Canada, T6G 2H7; †School of Pharmacy, University of Wisconsin, Madison, Wisconsin 53706; and ‡Department of Biochemistry, University of Toronto, Toronto, Ontario, Canada, M5S 1A8

Communicated by Joseph S. Fruton, June 21, 1982

ABSTRACT **Crystals of the molecular complex between the esterified tripeptide fragment of pepstatin and the aspartyl proteinase penicillopepsin are isomorphous with crystals of native penicillopepsin. The difference electron-density map at 1.8-Å resolution, computed by using the amplitude differences and refined phases of reflections from the crystal of native penicillopepsin, unambiguously showed the binding mode of isovaleryl-Val-Val-StaOEt, where StaOEt is the ethyl ester of statine [(4*S*,3*S*)-4-amino-3-hydroxyl-6-methylheptanoic acid]. In addition, a major conformational change in penicillopepsin involving the large β loop of residues from Trp-71 to Gly-83 (the so-called "flap" region) occurs as a result of this inhibitor binding. This structural movement provides the first confirmation of the importance of enzyme flexibility in the aspartyl proteinase mechanism. The 3-hydroxyl group of the Statine residue and the carbonyl oxygen atom of the ethyl ester are situated on either side of the approximate plane containing the hydrogen-bonded carboxyl groups of Asp-33 and Asp-213. The observed binding mode of the pepstatin tripeptide fragment is similar to that predicted for the binding of good substrates with penicillopepsin [James, M. N. G. (1980) *Can. J. Biochem.* 58, 251–271].**

Pepstatin is a naturally occurring inhibitor of aspartyl proteinases (1); it has the amino acid composition isovaleryl (Iva)-Val-Val-Sta-Ala-StaOH, in which Sta is the residue of statine [(4*S*,3*S*)-4-amino-3-hydroxyl-6-methylheptanoic acid] (2). The interaction of pepstatin with aspartyl proteases is characterized by small dissociation constants [i.e., 4.6×10^{-11} M with porcine pepsin (3) and 1.5×10^{-10} M with penicillopepsin (unpublished results)]. It has been suggested that part of its inhibitory nature is due to the presence of the central Sta residue that could mimic the tetrahedral transition state of a good substrate (4, 5). The chemical formula of pepstatin is:

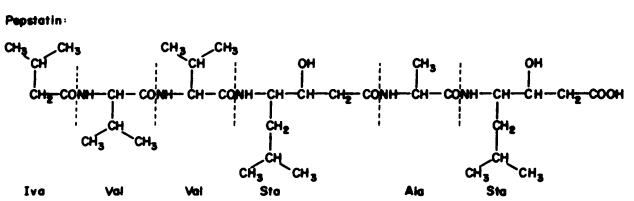

Structure I

Penicillopepsin is an aspartyl proteinase isolated from the mold *Penicillium janthinellum*. Its crystal structure (6, 7) has been refined at 1.8-Å resolution (8) to a conventional *R*-factor§ of 0.136 for those reflections with *I*, the intensity of Bragg reflections, equal to or greater than the estimated standard deviation of the intensity measurement derived from counting statistics [$I \geq \sigma(I)$]. The aspartyl proteinases are characterized by a long binding cleft that can accommodate 7 or 8 amino acid residues of an oligopeptide substrate in an extended conformation. The two catalytically important aspartyl residues, Asp-33 and Asp-213, are centrally located in this binding cleft (Asp-32 and Asp-215 in the porcine pepsin sequence numbering).

Fluorescence measurements on the aspartyl proteinases with specific substrates have indicated that conformational mobility of groups in the active site may play an important role in the mechanism of these enzymes (9).

MATERIALS AND METHODS

The enzyme, penicillopepsin, was prepared, purified, and crystallized as described (6, 7, 10). Crystals of the native enzyme (Fig. 1 *Left*) have space group *C*2 with unit cell dimensions of $a = 97.4$ Å, $b = 46.6$ Å, $c = 65.4$ Å, and $\beta = 115.4°$ ($Z = 4$ molecules per unit cell). Least-squares refinement of the initial model deduced at 2.8-Å resolution (6, 7) was done with the restrained parameter refinement program of Hendrickson and Konnert (11). Phases for the 21,962 reflections with $I \geq \sigma(I)$ at 1.8-Å resolution were calculated from the final refined model at an *R* value of 0.136 (8). This model included 319 solvent molecules in addition to the 2,363 atoms of the native enzyme.

The pepstatin derivative Iva-Val-Val-StaOEt was synthesized by the following procedure. *t*-Butoxycarbonyl (Boc)-StaOEt (12) was deprotected with 4 M HCl in dioxane and sequentially coupled with Boc-L-valine, Boc-L-valine, and isovaleryl anhydride by using procedures previously described for the synthesis of pepstatin analogues (13) to give the desired compound in about 35% overall yield. Physical characteristics: mp = 235–236°C; TLC $R_f = 0.52$ in chloroform/methanol, 9:1 (vol/vol); $\alpha_D^{24} = -80°$ ($c = 0.0585$, methanol). Analysis. Calculated for $C_{25}H_{47}N_3O_6$: C, 61.82; H, 9.76; N, 8.65. Found: C, 61.79; H, 9.77; N, 8.68. Iva-Val-Val-StaOEt inhibits penicillopepsin competitively with a $K_i \simeq 1.6 \times 10^{-9}$ M (unpublished data).

Previous experience with native crystals of penicillopepsin indicated that soaking them in solutions of various inhibitors or substrates had only limited success (6, 14, 15). The extremely limited solubility of the tripeptide inhibitor required that the complex be formed in 50% methanol buffer by slowly mixing 0.5 ml of 0.3 mM penicillopepsin/20 mM sodium acetate, pH 4.5, with an equal volume of 0.6 mM Iva-Val-Val-StaOEt in methanol, which was kept on dry ice. Penicillopepsin is stable in methanol/water, 1:1 (vol/vol), below 0°C (unpublished results). The mixture was subsequently dialyzed against several

The publication costs of this article were defrayed in part by page charge payment. This article must therefore be hereby marked "*advertisement*" in accordance with 18 U. S. C. §1734 solely to indicate this fact.

Abbreviations: Iva, isovaleryl; Sta, residue of statine [(4*S*,3*S*)-4-amino-3-hydroxyl-6-methylheptanoic acid]; Boc, *t*-butoxycarbonyl.

§ *R* is defined as $\Sigma||F_o| - |F_c||/\Sigma|F_o|$, where $|F_o|$ and $|F_c|$ are the observed and calculated structure factor amplitudes, respectively.

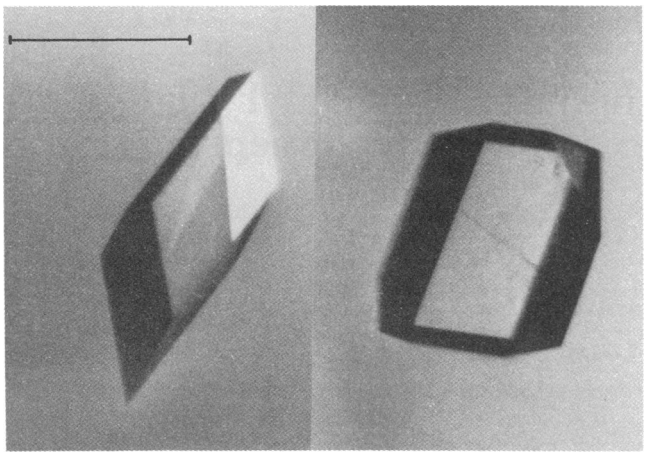

FIG. 1. (*Left*) Crystals of native penicillopepsin show an elongated habit. The long body diagonal of the crystals is a*. (Bar = 0.5 mm) (*Right*) A crystal of the complex of the pepstatin fragment Iva-Val-Val-StaOEt with penicillopepsin. The habit of these crystals is distinctly different from that of the native enzyme crystals, but they remain isomorphous. The magnification is the same as that in *Left*.

changes of ice-cold distilled water that had been adjusted to pH 4.5 with acetic acid. The complex was then freeze-dried and used directly in crystallization experiments at 10 mg/ml in 25% saturated $(NH_4)_2SO_4$/0.1 M Na acetate buffer, pH 4.4. Vapor diffusion by the hanging drop technique [reservoir, 40% saturated $(NH_4)_2SO_4$/0.1 M Na acetate, pH 4.4] was used. A crystal morphology different from that of the native enzyme (Fig. 1 *Left* and *Right*) was the first indication that the complex had crystallized. The relative growth of specific faces are clearly altered, while isomorphism is maintained. Similar observations with the complex of a trisaccharide bound to hen egg white lysozyme have been made (16).

The crystals of Iva-Val-Val-StaOEt complexed to penicillopepsin have unit cell dimensions a = 97.2 Å, b = 46.5 Å, c = 65.7 Å, and β = 115.1° and, thus, are isomorphous with crystals of the native enzyme. Intensity data collection was done with a Nonius CAD4 diffractometer, fitted with an extended counter arm (crystal–counter distance, 60 cm) and a He-filled diffracted beam tunnel. Ni-filtered CuK_α radiation (40 kV, 26 mA) was used for all measurements. Full ω angle scans of 1.2° were necessary for total peak and background measurements due to crystal splitting (up to 0.4° in ω). Absorption corrections were deduced from ψ scans (17) for two reflections. The falloff of intensity of the diffraction pattern due to radiation damage was corrected by a function of time and θ (18). In this way, ≈30,000 reflections were measured from one crystal of the complex during a period of 31 days. The maximum decay correction required for reflections with $\sin\theta/\lambda \simeq 0.264$ was 55%, whereas that for the data of low $\sin\theta/\lambda$ was only 15–20%.

The structure factor amplitudes of the crystal of the molecular complex were scaled to the absolute scale with the program ORESTES (19). The ratio of the sums of the structure factor amplitudes for the native and complex crystals was 0.941, and no further scaling corrections were made. The agreement index¶ between the two appropriately scaled data sets was 0.272. A difference electron-density map was computed from the coefficients $|F_{complex}| - |F_{native}|$ and phases α_{native}, which are the calculated phase angles for the refined structure of penicillopepsin (8). No attempt to omit the contribution of those waters occupying the immediate vicinity of the active site or neighboring substrate binding regions was made in calculating these phases.

The computed map was transferred to the MMS-X interactive graphics (20) at the University of Alberta. The program, M3, designed and developed by C. Broughton, was used for the display of the molecules, electron-density maps, and the animated models of the pepstatin tripeptide for electron-density fitting (21).

RESULTS AND DISCUSSION

There are only two prominent features in the difference electron-density map. They are readily interpreted as the bound tripeptide inhibitor and a major conformational change in a portion of the enzyme.

Inhibitor Conformation. The difference electron density for the pepstatin fragment Iva-Val-Val-StaOEt bound in the active site is shown in Fig. 2. With the exception of the terminal methyl groups of Iva-1, the model fits exceptionally well into the electron density. Some distortion of the electron density is to be expected because of the presence of solvent molecules in the native structure used in the phase calculations.

Table 1 lists the conformational angles for the residues of the pepstatin fragment. These values are the result of the electron-density fitting and, therefore, are almost certain to change upon refinement of the structure. The ϕ values for the backbone of the tripeptide are all close to that expected for an extended polypeptide chain (−120°), but only ψ of Val-2 is close to the expected +140°. Nevertheless, Fig. 2 shows the approximate β-sheet conformation adopted by the inhibitor with the side chains alternating to the left and to the right of the backbone. In this manner, a polypeptide of 7 or 8 amino acids could be accommodated into the active site of penicillopepsin. This observation agrees well with the kinetic data of Fruton and others, who first indicated an extended binding site for the aspartyl proteinases (23, 24).

The side-chain conformational angles, χ^i, for Val-3 and Sta-4 are well within the most commonly observed values and calculated energetic minima for valyl and leucyl residues, g^+ and g^+t (8, 22). It is of interest that the enzyme binds the inhibitor with no apparent distortion of this conformation in this most critical portion of the inhibitor molecule. The conformation of Val-2 (g^-) is different from that of Val-3 but also within accepted ranges.

Intermolecular Nonbonded Contacts. The conformation of the pepstatin tripeptide fragment and the relative orientation of this inhibitor serve to delineate the binding sites on the penicillopepsin molecule. For convenience we will use the notation of Schechter and Berger (25) to denote the residues on the substrate (in this case, the inhibitor) as P_1, P_2, and P'_1, P'_2, etc. The overall binding mode of the pepstatin tripeptide inhibitor is shown in Fig. 3. There are a total of 82 nonbonded contacts less than 4.0 Å (including hydrogen bonds) that the atoms of the tripeptide inhibitor make with atoms of the enzyme. Fifteen residues of penicillopepsin are engaged in these interactions. By far the largest number of contacts (40 of the total of 82) are made by the P_1 Sta residue to 10 residues of penicillopepsin. These residues are Asn-31, Asp-33, Gly-35, Leu-121, Asp-213, Gly-215, Thr-216, and, after the conformational movement of the "flap" (the β-sheet from Trp-71 to Gly-83), Tyr-75, Asp-77, and Ser-79. An alternative orientation for a P_1 lysyl residue having an ion-pair bond between N^ζ of the lysine and the carboxylate of Asp-38 has been proposed (15, 26) on the basis of model-building studies. A hydrogen bond from the nitrogen atom of the P_1 residue to the C=O of Gly-215 was proposed previously (26), also on the basis of model building, and is confirmed by

¶ Defined as $\Sigma||F_{complex}| - |F_{native}||/\frac{1}{2}\Sigma||F_{complex}| + |F_{native}||$.

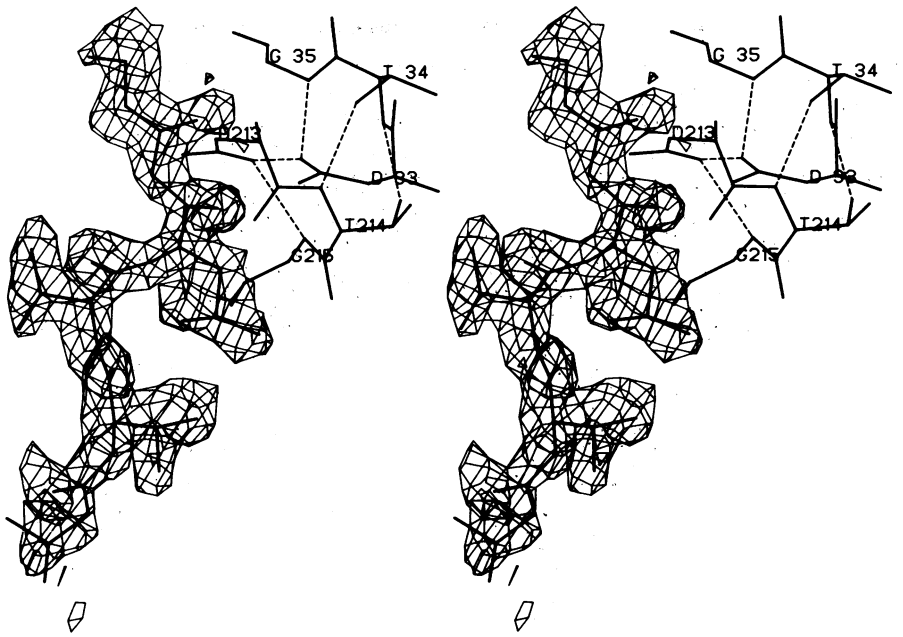

FIG. 2. A stereoscopic view of a portion of the difference electron-density map at 1.8-Å resolution in the vicinity of the active site of penicillopepsin. The two catalytically important aspartate residues are Asp-33 and Asp-213. The electron-density contour surface is drawn at +0.18e Å^{-3}, and the fitted Iva-Val-Val-StaOEt model is superimposed. Hydrogen bonds are denoted by dashed lines.

the conformation of Sta-4 in the present observed binding mode for the pepstatin fragment.

Residue Val-3 is the P_2 amino acid, and the major contacts are to the atoms of the flap, especially Asp-77. Two hydrogen bonds can be identified, one from the O^{δ} of Asp-77 to the NH of Val-3 and the other from either the NH of Gly-76 or the NH of Asp-77 (or both) to the C=O of Val-3. These latter hydrogen bonds can only be confirmed after least-squares refinement of the complex. They would represent very important interactions to position the scissile bond appropriately relative to the two aspartyl residues of the active site.

There are two key hydrogen bonds involving Val-2, the P_3 residue (Fig. 3). The main-chain NH of Val-2 donates a proton to the side chain O^{γ} of Thr-217, and the carbonyl oxygen atom accepts a proton from the peptide NH of Thr-217. There are relatively few nonbonded contacts involving the side-chain atoms of Val-2. There is a surface depression formed by the side chains of Glu-15 and Glu-16 at the bottom of the active-site cleft, that could be involved in binding a bulkier P_3 residue.

Table 1. Conformational angles for the pepstatin fragment*

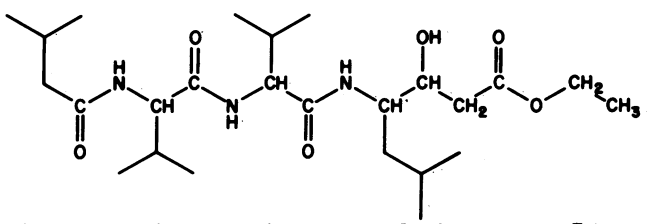

Residue	Angle, degree ϕ	ψ	χ^1	χ^2	Conformation†
Iva-1	—	72‡	48‡	—	*t*
Val-2	−117	149	−57	—	g^-
Val-3	−122	93	−171	—	g^+
Sta-4	−127	64‡	−54	−179	g^+t

* ϕ and ψ are conformational angles of the polypeptide chain: ϕ = CO_{i-1}—N_i—C_i^{α}—CO_i, ψ = N_i—C_i^{α}—CO_i—N_{i+1}.

† This nomenclature of side-chain conformation refers to the position of C_{γ}; g^-, *trans* to H^{α}; *t*, *trans* to the amino group; g^+, *trans* to the carbonyl group (22).

‡ The ψ and χ^1 values for Iva are based on a hypothetical position for an α-amino nitrogen atom. The ψ value for Sta-4 is defined by NH—C^{α}—CH—CH_2—. The small value of 64° is probably the result of the three bonded tetrahedral carbon atoms.

The carbonyl oxygen of the isovaleryl group makes no hydrogen-bonded interactions with proton donors on penicillopepsin. The methyl and methylene groups interact with Thr-217 and Leu-218. Minor conformational changes in penicillopepsin also could involve Leu-284 and Tyr-274 in these interactions, as the difference map seems to indicate.

The ethyl group of the ester occupies a hydrophobic pocket that has been identified as a probable S_1' binding site on penicillopepsin (26). Close contacts are made to Phe-190, Ile-211, and Phe-295. The CH_3 group could coincide with the position occupied by the P_1' Ala C^{β} atom in the intact pepstatin.

It can be seen from Figs. 2 and 3 that the

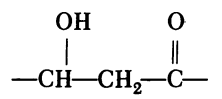

group of Sta-4 straddles the plane of the two carboxyl groups of Asp-33 and Asp-213. The tetrahedral nature of the 3-carbon atom of P_1 Sta is very clear from the difference map (Fig. 2). Its proximity to one of the O^{δ} atoms of Asp-33 causes a rotation of that carboxyl group away from the inhibitor. The hydroxyl oxygen atom does not exactly replace the solvent site, O-39, in the native enzyme (8), but that solvent is displaced in order to accommodate the inhibitor. Even though the direction of nucleophilic attack on the carbonyl carbon of a good substrate can be inferred from the present difference map (i.e., from a water bound to the carboxylate of Asp-33), we would prefer to await the unequivocal results expected from the least-squares refinement at 1.8-Å resolution of the complex data.

Enzyme Mobility. Gross conformational changes in the immediate vicinity of the active site of penicillopepsin so that the carboxylate of either Asp-33 or Asp-213 would become more accessible is unlikely (8, 14). This region is extensively and in-

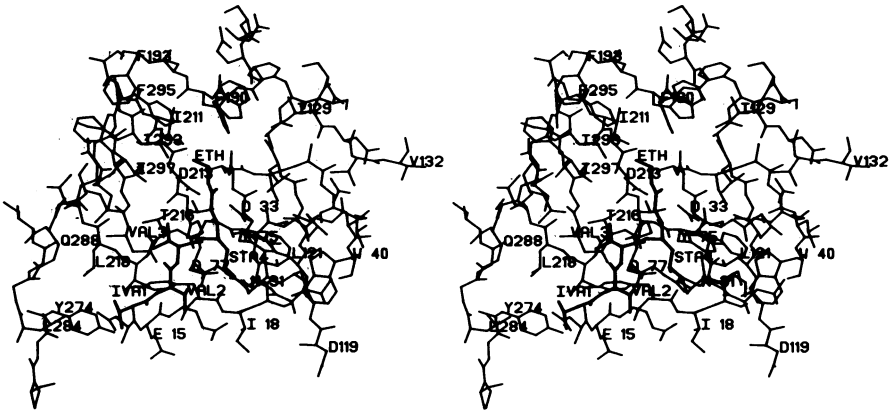

FIG. 3. The active-site region (in stereo) of native penicillopepsin at 1.8-Å resolution (8). Superimposed is the molecular model of the pepstatin fragment as deduced from the difference electron-density map (Fig. 2). The flap is shown in the position determined for the native enzyme crystals.

tricately hydrogen-bonded (see Fig. 2) and is the least mobile (or flexible) region of the molecule, as judged by the relatively low isotropic thermal *B* factors (8). However, conformational flexibility of some segment of the molecule close to the active site or binding region is indicated by many kinetic and substrate binding studies (9). It is not yet established that conformational flexibility is mandatory for the sequence of events that involve the covalency changes of peptide bond hydrolysis, and the present data would indicate that this is not necessary. However, mobility of the flap was suggested as one of the prerequisite steps to accommodate substrates in the extended binding clefts of the aspartyl proteases (14). The present study confirms this proposal and extends the interpretation of the possible role of this flap region in the hydrolytic and transpeptidation events. This segment of penicillopepsin undergoes a substantial change in conformation and its concerted movement is depicted in Fig. 4. It can be seen that residues from Trp-71 to Gly-83 lie in a continuous region of negative electron density on the difference map. This indicates that these residues do not have the same relative position in the complex as they do in the crystals of native, uncomplexed penicillopepsin. Indeed, lying adjacent to the negative density contour surface is a continuous stretch

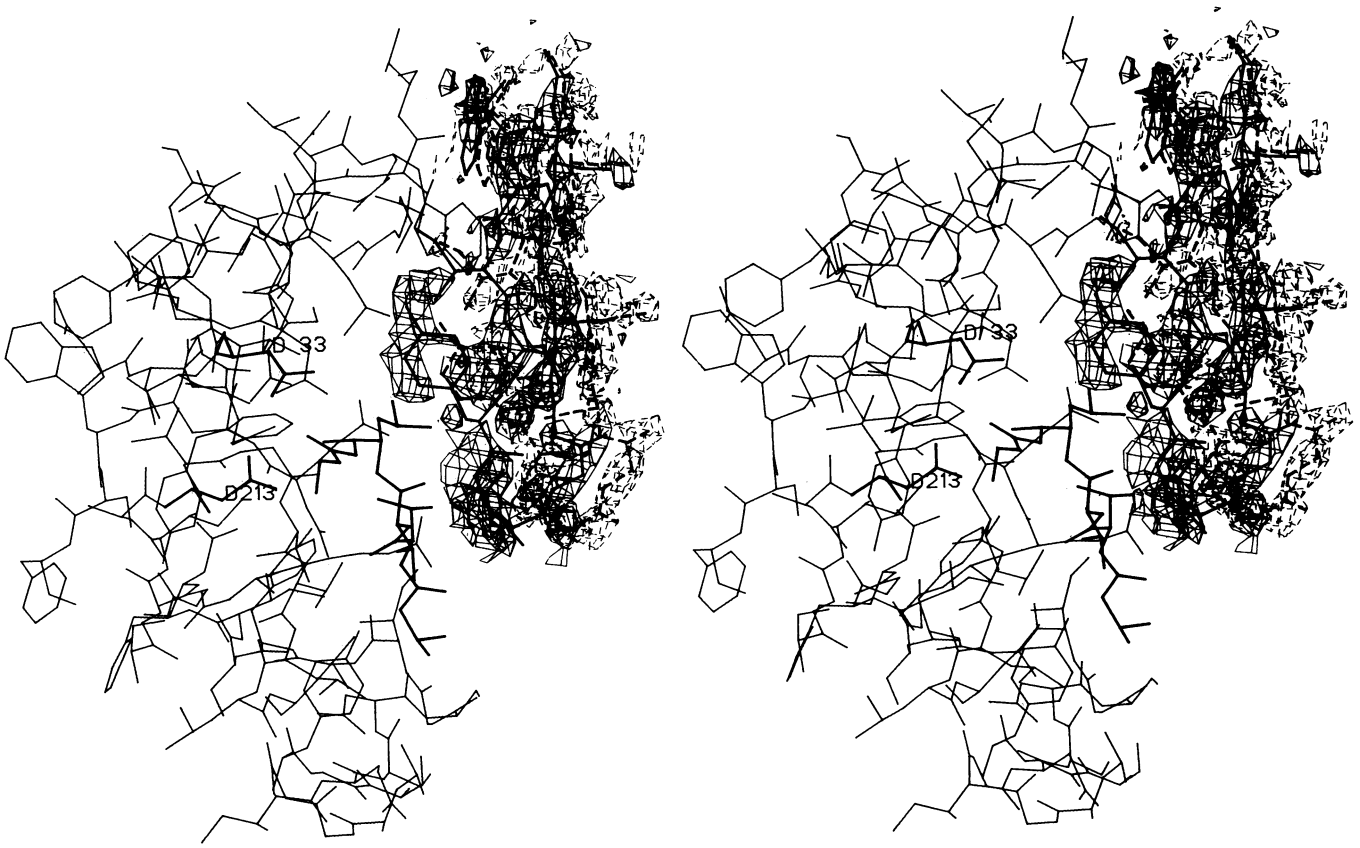

FIG. 4. The region of the difference electron-density map showing the large conformational movement of the flap. Negative contours ($-0.20e$ Å^{-3}) are dashed thin lines and coincide with the position of the residues of the flap in the native enzyme (thick dashed lines). The positive contours ($+0.20e$ Å^{-3}) are thin lines representing the final position to which the residues of the flap have moved (thick lines). The residues of Iva-Val-Val-StaOEt are shown in relation to this conformational movement. Asp-33 and Asp-213 are highlighted by thick lines. The remaining residues correspond to those shown in Fig. 3.

of positive electron density showing the new positions of these residues in the crystals of the complex. A molecular model of the β-sheet of this flap was animated in the MMS-X graphics, and the new position was attained by a hinge-like rotation around an axis connecting the C^{α} atoms of Trp-71 and Gly-83. The details of this very simple model of the movement will undoubtedly change upon refinement, but it accounts well for the appearance of the difference electron-density map (Fig. 4).

The far-reaching implications of this conformational change are numerous. The new position of the flap requires movement of atoms in the neighborhood of Gly-76 and Asp-77 by ≈2.2 Å. The side chain of Asp-77 and portions of the main chain in this region are brought into close proximity of the pepstatin inhibitor, thus permitting the formation of hydrogen bonds between atoms of the flap and the inhibitor. As these hydrogen bonds are exclusively to the polypeptide chain of the pepstatin tripeptide, side-chain specificity is not part of the interaction, and similar contacts and hydrogen bonds could also form with the backbone of a good substrate. These hydrogen-bonding interactions clearly help to position the scissile bond in the proper orientation relative to the catalytic apparatus of the aspartyl proteinases.

The movement of the flap eliminates the possible role of proton donor for the *p*-hydroxyl group of Tyr-75 (7, 14, 15, 26). An earlier study (7) that involved binding 1,2-epoxy-3-*p*-nitrophenoxypropane to penicillopepsin elicited a movement of the side chain of Tyr-75 towards the active site, suggesting that Tyr-75 played a role of proton donor to the leaving group nitrogen in the catalytic mechanism of aspartyl proteinases (15, 26). However, the present study shows that if the observed conformational change of the flap also takes place when a good substrate binds to penicillopepsin, then the side chain of Tyr-75 can only enhance the specific binding interactions to the P_1 side chain, which often exhibits an aromatic preference (24, 27).

Finally, conformational changes that involve the flap region of the molecule can begin to explain the acyl and amino transfers (24, 28, 29) that occur in transpeptidation reactions. Covalent intermediates are not likely in the aspartyl proteinase mechanism (7, 14, 15). Residues NH_2-terminal to the scissile bond (P_1 and P_2) would be kept preferentially in place after hydrolysis by the new interactions made with residues of the flap after its conformational change. The large differences in yields of amino transpeptidations between penicillopepsin (low yield) and porcine pepsin can possibly be accounted for by a four-residue insertion in pepsin after Asn-290 relative to penicillopepsin. These residues, Asp-Val-Pro-Thr, could adopt a conformation resembling a flap that could interact preferentially with residues P'_1, P'_2, and P'_3 of a substrate, thus providing an explanation for the efficiency of the amino-transfer reactions of pepsin. However, the conformational changes observed may not be sufficient to account for the failure of the intermediates in the transpeptidation reactions to exchange their acyl or amino moieties with the corresponding free amino acids in the reaction mixture (30).

We congratulate Prof. J. S. Fruton on the occasion of his 70th birthday. We thank Koto Hayakawa for her patience and expertise in growing crystals of this complex. Mae Wylie typed the manuscript. The research in Edmonton was supported by a grant from the Medical Research Council of Canada to the Group in Protein Structure and Function, in Toronto by a grant from the Medical Research Council to T.H., and in Wisconsin by Grant AM 20,100 from the National Institutes of Health.

1. Umezawa, H., Aoyagi, T., Morishima, H., Matzusaki, M., Hamada, H. & Takeuchi, T. (1970) *J. Antibiot.* **23**, 259–262.
2. Morishima, H., Takita, T. & Umezawa, H. (1972) *J. Antibiot.* **25**, 551–552.
3. Workman, R. J. & Burkitt, D. W. (1979) *Arch. Biochem. Biophys.* **194**, 157–164.
4. Marciniszyn, J., Jr., Hartsuck, J. A. & Tang, J. (1976) *J. Biol. Chem.* **251**, 7088–7094.
5. Marshall, G. R. (1976) *Fed. Proc. Fed. Am. Soc. Exp. Biol.* **35**, 2494–2501.
6. Hsu, I.-N., Delbaere, L. T. J., James, M. N. G. & Hofmann, T. (1977) *Nature (London)* **266**, 140–145.
7. Hsu, I.-N., Delbaere, L. T. J., James, M. N. G. & Hofmann, T. (1977) in *Acid Proteases, Structure, Function and Biology*, ed. Tang, J. (Plenum, New York), pp. 61–81.
8. James, M. N. G. & Sielecki, A. R. (1982) *J. Mol. Biol.*, in press.
9. Fruton, J. S. (1980) *Mol. Cell. Biochem.* **32**, 105–114.
10. Sodek, J. & Hofmann, T. (1971) *Methods Enzymol.* **19**, 372–396.
11. Hendrickson, W. A. & Konnert, J. H. (1980) in *Computing in Crystallography*, eds. Diamond, R., Ramaseshan, S. & Venkatesan, K. (Indian Acad. Sci., Int. Union of Crystallogr., Bangalore, India), pp. 13.01–13.23.
12. Rich, D. H., Sun, E. T. O. & Boparai, A. S. (1978) *J. Org. Chem.* **43**, 3624–3626.
13. Rich, D. H., Sun, E. T. O. & Ulm, E. (1980) *J. Med. Chem.* **23**, 27–33.
14. James, M. N. G., Hsu, I.-N. & Delbaere, L. T. J. (1977) *Nature (London)* **267**, 808–813.
15. James, M. N. G., Hsu, I.-N., Hofmann, T. & Sielecki, A. (1981) in *Structural Studies on Molecules of Biological Interest*, eds. Dodson, G., Glusker, J. P. & Sayre, D. (Clarendon, Oxford), pp. 350–389.
16. Kelly, J. A., Sielecki, A. R., Sykes, B. D., James, M. N. G. & Phillips, D. C. (1979) *Nature (London)* **282**, 875–878.
17. North, A. C. T., Phillips, D. C. & Mathews, F. S. (1968) *Acta Crystallogr., Sect. A* **24**, 351–359.
18. Hendrickson, W. A. (1976) *J. Mol. Biol.* **106**, 889–893.
19. Thiessen, W. E. & Levy, H. A. (1973) *J. Appl. Crystallogr.* **6**, 309.
20. Barry, C. D., Molnar, C. E. & Rosenberger, F. U. (1976) *Technical Memorandum No. 229* (Computer Systems Laboratory, Washington University, St. Louis, MO).
21. Sielecki, A. R., James, M. N. G. & Broughton, C. G. (1982) in *Computing Methods in Crystallography*, 12th International Congress of Crystallography, ed. Sayre, D. (Clarendon, Oxford), pp. 409–420.
22. Janin, J., Wodak, S., Levitt, M. & Maigret, B. (1978) *J. Mol. Biol.* **125**, 357–386.
23. Fruton, J. S. (1976) *Adv. Enzymol. Relat. Areas Mol. Biol.* **44**, 1–36.
24. Wang, T. T. & Hofmann, T. (1977) *Can. J. Biochem.* **55**, 286–294.
25. Schechter, I. & Berger, A. (1967) *Biochem. Biophys. Res. Commun.* **27**, 157–162.
26. James, M. N. G. (1980) *Can. J. Biochem.* **58**, 251–271.
27. Powers, J. C., Harley, A. D. & Myers, D. V. (1977) in *Acid Proteases, Structure, Function and Biology*, ed. Tang, J. (Plenum, New York), pp. 141–157.
28. Takahashi, M. & Hofman, T. (1975) *Biochem. J.* **147**, 549–563.
29. Newmark, A. & Knowles, J. R. (1975) *J. Am. Chem. Soc.* **97**, 3557–3559.
30. Wang, T. T. & Hofmann, T. (1976) *Biochem. J.* **153**, 691–699.